TRANSFER REACTIONS BETWEEN 18O IONS AND LIGHT NUCLEI

Y. Eyal, I. Dostrovsky, Z. Fraenkel

TRANSFER REACTIONS BETWEEN ^{18}O IONS AND LIGHT NUCLEI

Y. EYAL, I. DOSTROVSKY and Z. FRAENKEL

The Weizmann Institute of Science, Rehovot, Israel

Résumé. — Les sections efficaces expérimentales des réactions de transfert de deux neutrons ^{18}O(^{18}O, ^{20}O)^{16}O et ^{14}C(^{18}O, ^{20}O)^{12}C sont comparées aux sections efficaces des réactions de transfert d'un neutron correspondantes. Aux énergies incidentes proches de la barrière coulombienne, on observe des sections efficaces considérablement plus grandes pour les réactions de transfert de deux neutrons. Les fonctions d'excitation et les distributions angulaires expérimentales de la réaction de transfert de deux neutrons ^{26}Mg(^{18}O, ^{16}O)^{28}Mg sont comparées à des calculs faits dans le cadre de l'approximation de Born avec ondes déformées et du modèle diffractionnel.

Abstract. — The experimental ^{18}O(^{18}O, ^{20}O)^{16}O and ^{14}C(^{18}O, ^{20}O)^{12}C 2-neutron transfer reaction cross sections are compared with the corresponding single-neutron transfer reactions. The 2-neutron transfer reactions are found to have a considerably larger cross section at bombarding energies near the Coulomb barrier. The experimental excitation function and angular distribution of the ^{26}Mg(^{18}O, ^{16}O)^{28}Mg 2-neutron transfer reaction are compared to calculations based on the DWBA method and the diffraction model.

In figure 1 we show the excitation functions for the 2-neutron transfer reaction ^{18}O(^{18}O, ^{20}O)^{16}O, the single-neutron transfer reaction ^{18}O(^{18}O, ^{19}O)^{17}O and the triton transfer reaction ^{18}O(^{18}O, ^{15}N)^{21}F. These reactions were measured by bombarding a thin (75 μg/cm^2 oxygen) target of highly enriched (98 % ^{18}O) tantalum oxide on 21 mg/cm^2 tantalum backing with ^{18}O ions. The reaction products were stopped in the tantalum backing and the ^{19}O, ^{20}O and ^{21}F formation cross sections were determined on the basis of the gamma ray energy and half life of these nuclides. In figure 2 we show the experimental excitation functions for the reactions ^{14}C(^{18}O, ^{16}O)^{16}C ; ^{14}C(^{18}O, ^{20}O)^{12}C ; ^{14}C(^{18}O, ^{19}O)^{13}C and ^{14}C(^{18}O, ^{15}N)^{17}N. These cross sections were determined by bombarding a 125 μg/cm^2 thick enriched (83 % ^{14}C)^{14}C-polyacetylene target on 245 mg/cm^2 gold backing with ^{18}O ions. The ^{14}C(^{18}O, ^{20}O)^{12}C and ^{14}C(^{18}O, ^{19}O)^{13}C cross sections were again determined through the measurement of the ^{19}O and ^{20}O gamma activity whereas the cross sections of the remaining two reactions were measured by counting the delayed neutron activity of the ^{17}N and ^{16}C reaction products with a BF$_3$-paraffin neutron counter. Since the detailed decay scheme of ^{16}C is unknown we have assumed that one delayed neutron is emitted per disintegration of ^{16}C. Unlike the case of the ^{18}O + ^{18}O reaction the transferred clusters are not uniquely determined by the reaction products in the ^{18}O + ^{14}C reactions. Yet one may assume that the ^{14}C(^{18}O, ^{20}O) ^{12}C and ^{14}C(^{18}O, ^{19}O)^{13}C reactions are essentially pure 2-neutron and single-neutron transfer

reactions respectively since the alternative possibility (^{6}He and ^{5}He transfer) involves the transfer of much heavier and more strongly bound clusters. Moreover, the comparison of figures 1 and 2 shows a great similarity of the (^{18}O, ^{20}O) and (^{18}O, ^{19}O) excitation functions for the two targets. The most important conclusion which may therefore be drawn from the experimental results of figures 1 and 2 is that for both the ^{18}O + ^{18}O and the ^{18}O + ^{14}C reaction channels the 2-neutron transfer reactions cross section is considerably larger than the single-

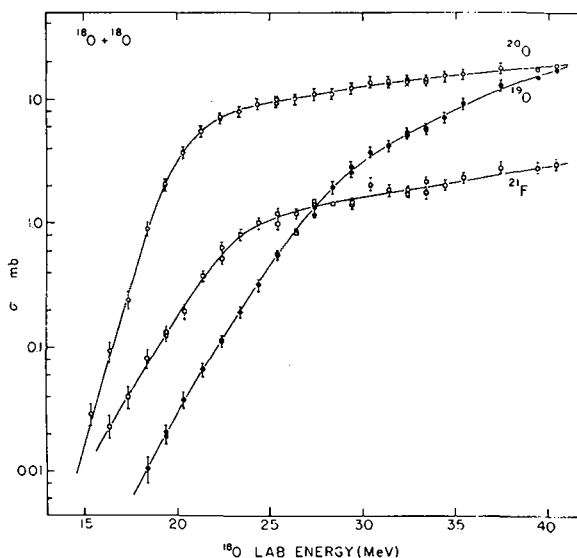Fig. 1. — Excitation functions for ^{19}O, ^{20}O, and ^{21}F from the reaction ^{18}O + ^{18}O.
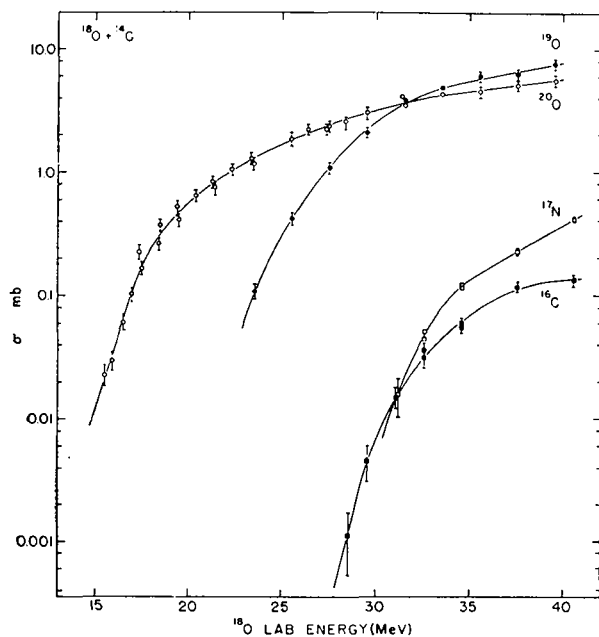
FIG. 2. — Excitation functions for ^{16}C, ^{17}N, ^{19}O and ^{20}O from the reaction $^{18}O + ^{14}C$.

FIG. 3. — Experimental excitation functions of $^{18}O(^{18}O, ^{20}O)^{16}O$ and $^{26}Mg(^{18}O, ^{16}O)^{28}Mg$ below the Coulomb barrier. The solid curves are results of calculations based on theory of Buttle and Goldfarb [1] .

neutron transfer reaction cross section at bombarding energies in the neighborhood of the Coulomb barrier (22-24 MeV). This indicates that the two neutrons are transformed as a correlated pair, most likely with zero angular momentum. In figure 3 the excitation function of $^{18}O(^{18}O, ^{20}O)^{16}O$ below the Coulomb barrier is compared with the results of a calculation based on the DWBA method of Buttle and Goldfarb [1] (solid line). These authors calculate the cross section for single neutron transfer between heavy ions at bombarding energies below the Coulomb barrier. Since in our case the reaction products ^{16}O and ^{20}O are probably mainly produced in their ground states we have used the formula which applied to zero angular momentum transfer [1]. The absolute value of the calculated curve has been normalized to experimental results. It is seen in figure 3 that despite the fact that in our reactions two neutrons rather than one are transferred between the heavy ions, the shape of the calculated curve fits that of the experimental results reasonably well.

In figure 3 are also shown the experimental and calculated excitation functions for the 2-neutron transfer reaction $^{26}Mg(^{18}O, ^{16}O)^{28}Mg$. The experimental reaction cross sections were obtained by bombarding natural magnesium targets 100-1 200 μg/cm² thick on 25 mg/cm² nickel backing with ^{18}O ions. The ^{28}Mg which was completely stopped in the target or backing was later separated radiochemically and the activity of the daughter nucleus ^{28}Al was measured by the β-γ coincidence method. For the calculated curve we used the same formula as was used for the $^{18}O(^{18}O, ^{20}O)^{16}O$ reaction. However, in the present case the assumption of zero angular-momentum transfer is not justified
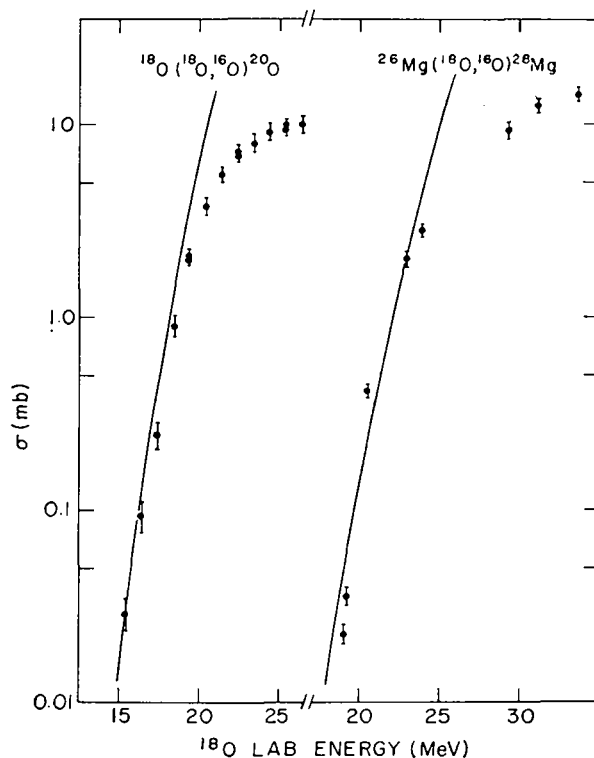
since a sizeable fraction the ^{28}Mg is created in its first excited state (1.468 MeV, 2^+). This is explained by the fact that unlike the Q-value for the $^{18}O(^{18}O,^{20}O)^{16}O$ reaction which is negative for all final states, the Q-value for the $^{26}Mg(^{18}O, ^{16}O)^{28}Mg$ is positive for the two first states of ^{28}Mg (assuming ^{16}O in its ground state). It is seen in figure 3 that indeed the shape of the calculated curve (which has been arbitrarily normalized to one experimental point) does not fit the experimental results.

In figures 4 and 5 we show the experimental angular distribution for the $^{26}Mg(^{18}O, ^{16}O)^{28}Mg$ reaction to given final states at two bombarding energies. These results were obtained by bombarding enriched (99.4 % ^{26}Mg) magnesium targets of 80-100 μg/cm² thickness on 15 μg/cm² carbon backings with an ^{18}O beam and detecting the two reactions products in two solid state detectors in coincidence. The most surprising result is the substantial fine structure in the angular distribution at the ^{18}O laboratory energy of 33.5 MeV and the absence of the sizable structure at 35.7 MeV. We have tried to fit the diffraction model of Dar and Koslovsky [2] to the experimental angular distribution. The results are shown in the solid lines of figures 4 and 5. The calculations have been normalized to the experimental results by a least square fit. Whereas the 35.7 MeV data could be fitted with
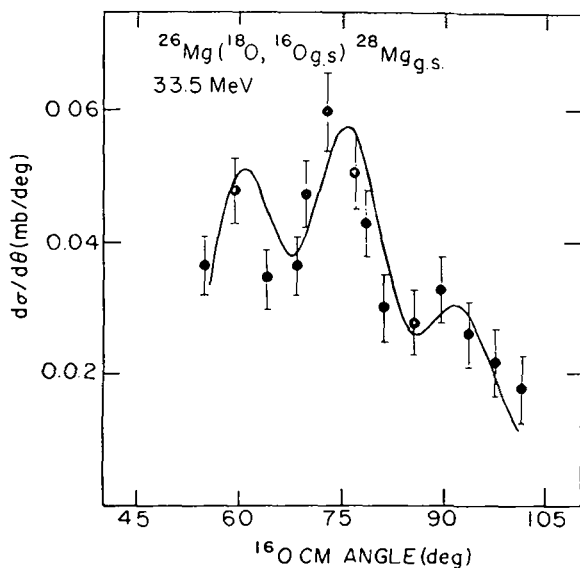
Fig. 4. — Center of mass angular distribution of ¹⁶O from the reaction ²⁶Mg(¹⁸O, ¹⁶O$_{g.s.}$) ²⁸Mg$_{g.s.}$ at ¹⁸O laboratory energy of 33.5 McV determined by the coincidence method. The curve represents results of calculation by the diffraction model.

and the « diffuseness parameters » d (d = 0.025 F) in order to fit the 33.5 MeV data (other parameters used : θ_0 = 72°, r_0 = 1.69 F).
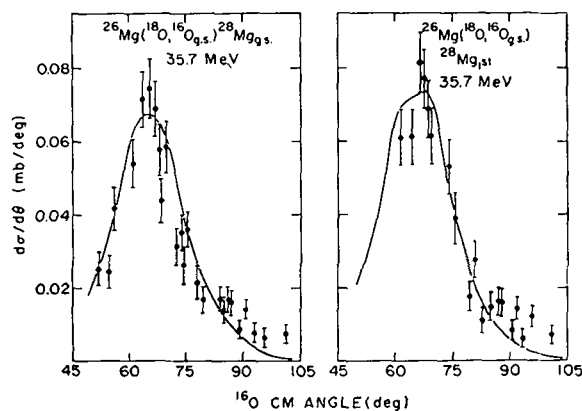

Fig. 5. — Center of mass angular distributions of ¹⁶O from the reactions ²⁶Mg(¹⁸O, ¹⁶O$_{g.s.}$) ²⁸Mg$_{g.s.}$ and ²⁶Mg(¹⁸O, ²⁶O$_{g.s.}$) ²⁸Mg$_1$st at ¹⁸O laboratory energy of 35.7 MeV determined by the coincidence method. The curves represent results of calculations by the diffraction model.

a « reasonable » set of parameters (θ_0 = 66°, r_0 = 1.60 F, L_0 = 16 and d = 0.35 F (for definitions and details see [2]) we had to use unreasonably low values for the cut-off angular momentum L_0 (L_0 = 9)

References

[1] BUTTLE (P. J. A.) and GOLDFARB (L. J. B.), Nucl. Phys., 1966, 78, 409.
[2] DAR (A.) and KOZLOWSKY (B.), Phys. Rev. Letters, 1965, 15, 1036.